

Provided for non-commercial research and education use.
Not for reproduction, distribution or commercial use.



This article appeared in a journal published by Elsevier. The attached copy is furnished to the author for internal non-commercial research and education use, including for instruction at the authors institution and sharing with colleagues.

Other uses, including reproduction and distribution, or selling or licensing copies, or posting to personal, institutional or third party websites are prohibited.

In most cases authors are permitted to post their version of the article (e.g. in Word or Tex form) to their personal website or institutional repository. Authors requiring further information regarding Elsevier's archiving and manuscript policies are encouraged to visit:

<http://www.elsevier.com/copyright>

Contents lists available at [SciVerse ScienceDirect](http://www.elsevier.com/locate/matresbu)

Materials Research Bulletin

journal homepage: www.elsevier.com/locate/matresbu

Improved photoluminescence properties of a new green $\text{SrB}_2\text{O}_4:\text{Tb}^{3+}$ phosphor by charge compensation

Zhan-Chao Wu^{*}, Ping Wang, Jie Liu, Chao Li, Wen-Hui Zhou, Shao-Ping Kuang^{*}

State Key Laboratory Base of Eco-Chemical Engineering, College of Chemistry and Molecular Engineering, Qingdao University of Science and Technology, Qingdao 266042, PR China

ARTICLE INFO

Article history:

Received 17 June 2012

Accepted 20 July 2012

Available online 27 July 2012

Keywords:

- A. Optical materials
- B. Chemical synthesis
- C. X-ray diffraction
- D. Luminescence
- D. Optical properties

ABSTRACT

A new green-emitting $\text{SrB}_2\text{O}_4:\text{Tb}^{3+}$ phosphor was synthesized by solid-state reaction. X-ray powder diffraction (XRD) analysis confirmed all the samples with orthorhombic formation of SrB_2O_4 . The excitation spectra indicate the phosphor can be effectively excited by near ultraviolet (NUV) light, making it attractive as conversion phosphor for LED applications. The phosphor exhibits a bright green emission with the highest photoluminescence (PL) intensity at 544 nm excited by 378 nm light. The critical quenching concentration of Tb^{3+} in $\text{SrB}_2\text{O}_4:\text{Tb}^{3+}$ is about 10 mol%. The effects of charge compensators (Li^+ , Na^+ , and K^+) on photoluminescence of $\text{SrB}_2\text{O}_4:\text{Tb}^{3+}$ were also studied. The results show that the emission intensity can be improved by all the three charge compensators and Na^+ is the optimal one for $\text{SrB}_2\text{O}_4:\text{Tb}^{3+}$. All properties show that the phosphor is a promising green phosphor pumped by NUV InGaN chip for fabricating white light-emitting diodes (WLEDs).

© 2012 Elsevier Ltd. All rights reserved.

1. Introduction

Compared with conventional illumination equipment, white light-emitting diodes (WLEDs) have several advantages such as high luminous efficiency, low power consumption, maintenance and environmental protection [1–3]. There are two methods for fabricating WLEDs (blue chip + yellow phosphor and near-ultraviolet (NUV) chip + tricolor (red, green, and blue) phosphors). WLEDs fabricated with NUV chips (350–410 nm) and tricolor (red, green, and blue) phosphors have higher color rendering index than that of present commercial WLEDs fabricated with blue chips and yellow phosphors $\text{YAG}:\text{Ce}^{3+}$, because all the colors are determined by the phosphors [4,5]. So the former fabrication process is proposed. However, the main tricolor phosphors for NUV InGaN-based LEDs are still some classical phosphor, such as $\text{BaMgAl}_{10}\text{O}_{17}:\text{Eu}^{2+}$ for blue, $\text{ZnS}:(\text{Cu}^+, \text{Al}^{3+})$ for green, and $\text{Y}_2\text{O}_2\text{S}:\text{Eu}^{3+}$ for red [6]. Especially, $\text{ZnS}:(\text{Cu}^+, \text{Al}^{3+})$ and $\text{Y}_2\text{O}_2\text{S}:\text{Eu}^{3+}$ are sulfide-based phosphors which exhibit low chemical stabilities against strong irradiation from InGaN chip and cause some environmental problems both in preparation and in application as they contain toxic elements. Therefore, it is urgent to search for new green and red phosphors with high efficiency, excellent stability, no environmental hazards and good chromaticity coordinates.

Borate is excellent matrices for luminescent materials for several advantages such as low synthetic temperature, high stability, high luminescence efficiency and cheap raw materials. During the past few years, a number of red and green emitting borate phosphors have been synthesized and studied extensively which can be used for fabricating WLEDs [7–14]. However, to the best of our knowledge, there is no report about the green $\text{SrB}_2\text{O}_4:\text{Tb}^{3+}$ phosphor for potential application on WLEDs.

In this paper, a new green phosphor $\text{SrB}_2\text{O}_4:\text{Tb}^{3+}$ was synthesized by solid stated reaction technique and its photoluminescent properties were investigated. For $\text{SrB}_2\text{O}_4:\text{Tb}^{3+}$ phosphor, Tb^{3+} ions is expected to replace Sr^{2+} ions in the host lattice, which would be difficult to keep charge balance in the crystallite sample. Hence, doping univalent charge compensator (Li^+ , Na^+ and K^+) is necessary to keep the charge balance. However, little attention has been paid to the effect of charge compensation on the luminescent properties of green-emitting borate phosphors. Therefore, in this paper, we focused our work on the effects of charge compensators on the photoluminescence properties of $\text{SrB}_2\text{O}_4:\text{Tb}^{3+}$.

2. Experimental

2.1. Samples preparation

The $\text{Sr}_{1-x}\text{B}_2\text{O}_4:\text{Tb}^{3+}_x$ ($x = 0.00, 0.02, 0.06, 0.10, 0.14, 0.18$) samples were prepared by a conventional solid-state reaction technique. Because Tb^{3+} ions are located in Sr^{2+} sites and some charge defect is built into the lattices, Li^+ , Na^+ or K^+ was added as

^{*} Corresponding authors. Tel.: +86 532 84023653; fax: +86 532 84023927.
E-mail addresses: wuzhan_chao@163.com (Z.-C. Wu), qustksp@126.com (S.-P. Kuang).

charge compensator. Thus, a series of $\text{Sr}_{1-2x}\text{B}_2\text{O}_4:\text{Tb}^{3+}_x\text{M}^+_{1-x}$ ($x = 0.02, 0.06, 0.10, 0.14, \text{ and } 0.18$; $\text{M} = \text{Li}, \text{Na}, \text{ and } \text{K}$) samples were also prepared by a same method as a comparison. The starting materials are SrCO_3 (AR), Li_2CO_3 (AR), Na_2CO_3 (AR), K_2CO_3 (AR), B_2O_3 (AR), and Tb_4O_7 (99.99%). The appropriate amount of starting materials were ground thoroughly, and then burned in an electric furnace at 800°C for 6 h.

2.2. Measurements

Crystal phase identification was carried out on an X-ray diffractometer (D-MAX2500/PC, RIGAKU Corporation of Japan) using 40 kV, 20 mA, and $\text{Cu K}\alpha$ radiation (1.5406 \AA). Morphology and size of the calcined particles were observed by field-emission scanning electron microscopy (FE-SEM, JSM-6700F, JEOL Corporation of Japan). Excitation and emission spectra of the powdered phosphors were measured by a fluorescence spectrometer (F-2700, HITACHI High-Technologies Corporation) and a 450 W xenon lamp was used as the excitation source. All measurements were made at room temperature unless otherwise stated.

3. Results and discussion

3.1. XRD of phosphor powders

The XRD patterns of $\text{Sr}_{0.90}\text{B}_2\text{O}_4:\text{Tb}^{3+}_{0.10}$ and $\text{Sr}_{0.80}\text{B}_2\text{O}_4:\text{Tb}^{3+}_{0.10}\text{M}^+_{0.10}$ ($\text{M}^+ = \text{Li}^+, \text{Na}^+ \text{ and } \text{K}^+$) are shown in Fig. 1. From Fig. 1, it can be observed that the four compounds have similar features and agree well with the Joint Committee on Powder Diffraction Standards (PDF 15-0779), indicating that the doped Tb^{3+} and charge compensators had not caused obvious change in the host structure. The crystal structure of SrB_2O_4 can be refined to be orthorhombic, space group $Pnca$ with $a = 6.589$, $b = 12.018$ and $c = 4.3373$.

3.2. FE-SEM images of phosphor powders

Fig. 2 shows the FE-SEM image of $\text{Sr}_{0.90}\text{B}_2\text{O}_4:\text{Tb}^{3+}_{0.10}$ powders. It was observed that the microstructure of the phosphor consisted of irregular grains with smooth surface. The average size of the $\text{Sr}_{0.90}\text{B}_2\text{O}_4:\text{Tb}^{3+}_{0.10}$ powders is about 2–6 μm . The results show that $\text{SrB}_2\text{O}_4:\text{Tb}^{3+}$ phosphor has a good crystallinity and a relatively low sinter temperature, which is also consistent with the requirements of energy saving for products in today's society.

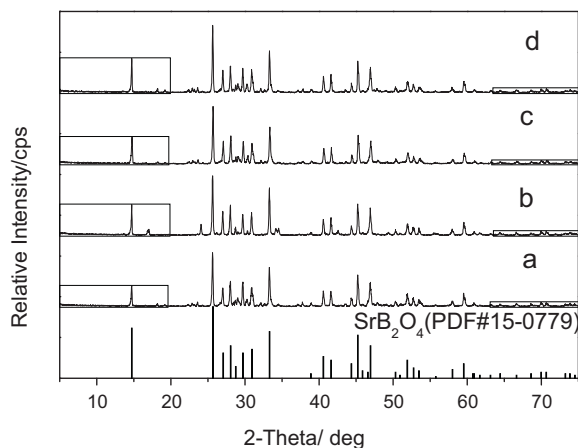


Fig. 1. XRD patterns of samples (a: $\text{Sr}_{0.90}\text{B}_2\text{O}_4:\text{Tb}^{3+}_{0.10}$; b: $\text{Sr}_{0.80}\text{B}_2\text{O}_4:\text{Tb}^{3+}_{0.10}\text{Li}^+_{0.10}$; c: $\text{Sr}_{0.80}\text{B}_2\text{O}_4:\text{Tb}^{3+}_{0.10}\text{Na}^+_{0.10}$; d: $\text{Sr}_{0.80}\text{B}_2\text{O}_4:\text{Tb}^{3+}_{0.10}\text{K}^+_{0.10}$).

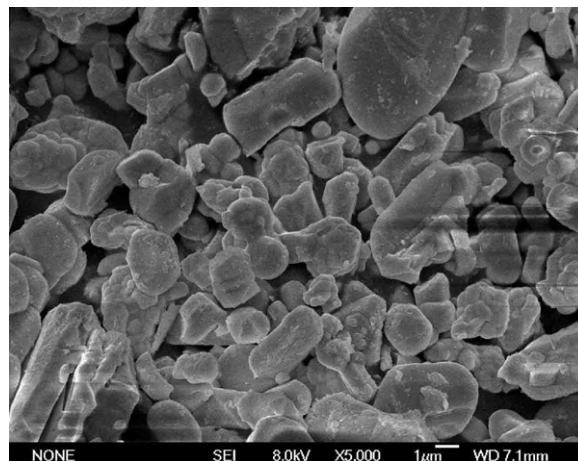


Fig. 2. FE-SEM images of $\text{Sr}_{0.90}\text{B}_2\text{O}_4:\text{Tb}^{3+}_{0.10}$.

3.3. Photoluminescence properties

The excitation spectrum of $\text{Sr}_{0.90}\text{B}_2\text{O}_4:\text{Tb}^{3+}_{0.10}$ monitored at 544 nm is shown in Fig. 3. The spectrum clearly indicates several excitation peaks at 319, 353, 370 and 378 nm, which can be ascribed to the transitions from 7F_6 to 5D_J , 5G_J , $^5L_{10}$ and 5D_3 of Tb^{3+} , respectively. In addition, $\text{SrB}_2\text{O}_4:\text{Tb}^{3+}$ shows intense $f \rightarrow f$ transition absorption, which may be attributed to the uneven components mix a small amount of opposite parity wave functions (e.g., $5d$) into $4f$ wave functions. So the parity selection rule is relaxed [15].

Tb^{3+} ion with $4f^8$ configuration has complicated energy levels, so its emission spectrum consisting of many peaks due to $^5D_J \rightarrow ^7F_J$ transitions should be observed. Fig. 4 is the emission spectrum of $\text{Sr}_{0.90}\text{B}_2\text{O}_4:\text{Tb}^{3+}_{0.10}$ excited by 378 nm NUV light. At 378 nm excitation, the emission spectrum exhibits four major emission peaks at 490, 544, 584 and 622 nm, which are attributed to the $^5D_4 \rightarrow ^7F_6$, $^5D_4 \rightarrow ^7F_5$, $^5D_4 \rightarrow ^7F_4$ and $^5D_4 \rightarrow ^7F_3$ typical transitions of Tb^{3+} , respectively. The strongest emission peak appears at 544 nm. The reason for this phenomenon may be due to the largest probability for both electric-dipole and magnetic-dipole induced transitions [16]. The four typical emission peaks are splitted in different degree. These splits maybe result from the crystal field effects, and their split extent is related to the structure characteristic of SrB_2O_4 crystal field.

Effects of Tb^{3+} concentration on the emission spectra of $\text{SrB}_2\text{O}_4:\text{Tb}^{3+}$ phosphors are also investigated. The emission spectra of $\text{SrB}_2\text{O}_4:\text{Tb}^{3+}$ phosphors prepared at various concentrations of Tb^{3+} ($x = 0.02, 0.06, 0.10, 0.14$ and 0.18) excited by 378 nm light and the dependence of photoluminescence intensity of

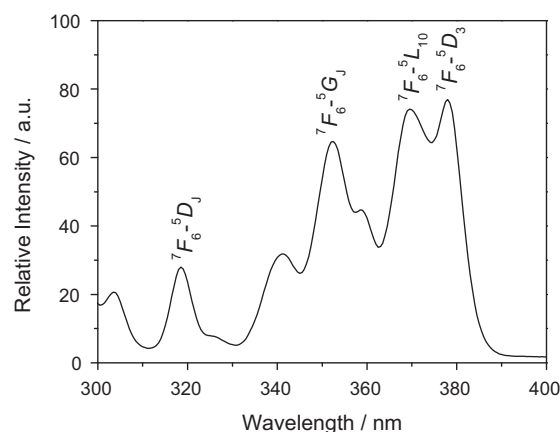


Fig. 3. Excitation spectra of $\text{Sr}_{0.90}\text{B}_2\text{O}_4:\text{Tb}^{3+}_{0.10}$ ($\lambda_{\text{em}} = 544 \text{ nm}$).

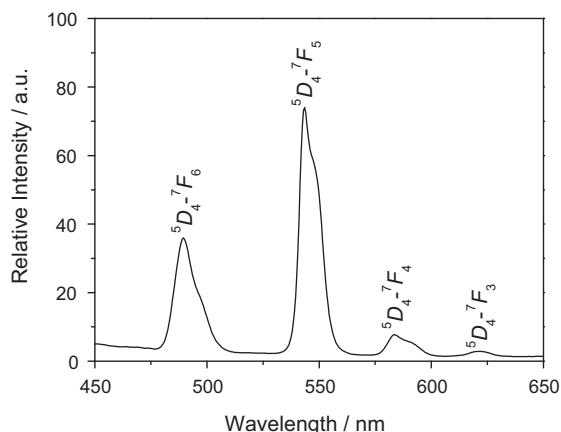


Fig. 4. Emission spectra of $\text{Sr}_{0.90}\text{B}_2\text{O}_4:\text{Tb}^{3+}_{0.10}$ ($\lambda_{\text{ex}} = 378 \text{ nm}$).

$\text{Sr}_{1-x}\text{B}_2\text{O}_4:\text{Tb}^{3+}_x$ on doped- Tb^{3+} concentration are given in Fig. 5. The photoluminescence intensity increases with Tb^{3+} -concentration increasing until a maximum intensity is reached, and then it decreases due to concentration quenching. The critical quenching concentration of Tb^{3+} is defined as the concentration at which the emission intensity begins to decrease. From Fig. 5, it can be found that the critical quenching concentration of Tb^{3+} in $\text{SrB}_2\text{O}_4:\text{Tb}^{3+}$ phosphor is about 10 mol%.

3.4. Effect of charge compensation on $\text{SrB}_2\text{O}_4:\text{Tb}^{3+}$ luminescence intensity

In the $\text{SrB}_2\text{O}_4:\text{Tb}^{3+}$ crystallite, Tb^{3+} ion is expected to replace Sr^{2+} ion. However, it would be difficult to keep charge balance in the samples. Therefore, univalent charge compensator (Li^+ , Na^+ or K^+) was added as charge compensators in order to keep the charge balance. Fig. 6 shows the effect of different charge compensators on the emission intensity of $\text{SrB}_2\text{O}_4:\text{Tb}^{3+}$. It is found that all the three charge compensators increase the emitting intensity of $\text{SrB}_2\text{O}_4:\text{Tb}^{3+}$. Na^+ ions exhibit the strongest charge compensation abilities, K^+ ions being the second, and Li^+ ions are the third. For example, the $^5\text{D}_4 \rightarrow ^7\text{F}_5$ emitting intensity of the sample with Na^+ ions as charge compensators is 4.36 times as strong as the one without charge compensator, 3.27 times for K^+ ions as charge compensators, and 2.80 times for Li^+ ions as charge compensators. The relative intensity ratios of $^5\text{D}_4 \rightarrow ^7\text{F}_5$ transition and CIE chromaticity coordinates of these phosphors are listed in

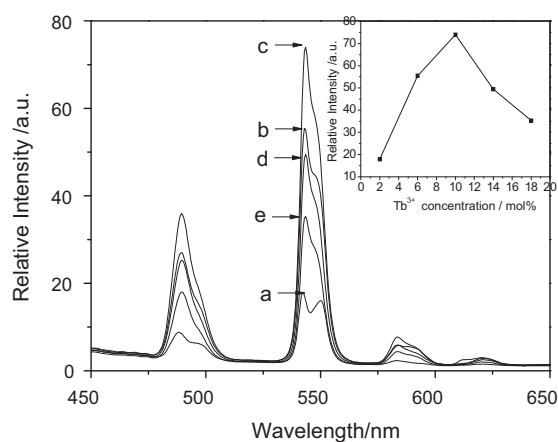


Fig. 5. Emission spectra of $\text{Sr}_{1-x}\text{B}_2\text{O}_4:\text{Tb}^{3+}_x$ with varying Tb^{3+} concentrations (a: $x = 0.02$; b: $x = 0.06$; c: $x = 0.10$; d: $x = 0.14$; e: $x = 0.18$) ($\lambda_{\text{ex}} = 378 \text{ nm}$). Inset: the dependence of photoluminescence intensity of $\text{Sr}_{1-x}\text{B}_2\text{O}_4:\text{Tb}^{3+}_x$ on Tb^{3+} concentration.

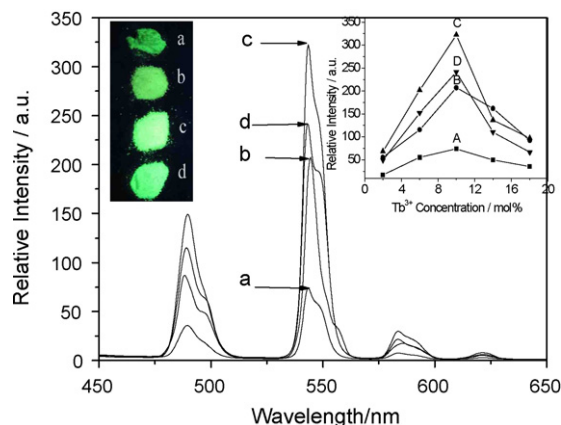


Fig. 6. Effect of different charge compensation on the emission intensity of $\text{SrB}_2\text{O}_4:\text{Tb}^{3+}$ (a: $\text{SrB}_2\text{O}_4:\text{Tb}^{3+}$; b: $\text{SrB}_2\text{O}_4:\text{Tb}^{3+},\text{Li}^+$; c: $\text{SrB}_2\text{O}_4:\text{Tb}^{3+},\text{Na}^+$; d: $\text{SrB}_2\text{O}_4:\text{Tb}^{3+},\text{K}^+$). Inset: the dependence of photoluminescence intensity of the samples on Tb^{3+} and charge compensators concentrations (A: $\text{Sr}_{1-x}\text{B}_2\text{O}_4:\text{Tb}^{3+}_x$; B: $\text{Sr}_{1-2x}\text{B}_2\text{O}_4:\text{Tb}^{3+}_x,\text{Li}^+_{0.10}$; C: $\text{Sr}_{1-2x}\text{B}_2\text{O}_4:\text{Tb}^{3+}_x,\text{Na}^+_{0.10}$; D: $\text{Sr}_{1-2x}\text{B}_2\text{O}_4:\text{Tb}^{3+}_x,\text{K}^+_{0.10}$).

Table 1. From Table 1, it can be seen that all the phosphors show excellent CIE Chromaticity coordinates which are closer to the phase alternation line (PAL) standard values ($x = 0.29$, $y = 0.60$). Especially, the CIE Chromaticity coordinates ($x = 0.27$, $y = 0.59$) of $\text{Sr}_{0.80}\text{B}_2\text{O}_4:\text{Tb}^{3+}_{0.10},\text{Na}^+_{0.10}$ are more closer to PAL standard values than those of others samples.

The emitting-intensity dependence relations of the samples on Tb^{3+} and charge compensators concentrations were also investigated (inset in Fig. 6). It can be seen that concentration quenching phenomena appear in all the four series samples. Namely, the photoluminescence intensity increases with Tb^{3+} and charge compensators concentrations increasing until a maximum intensity is reached, and then it decreases for all the four series phosphors. The critical quenching concentrations for all the four series phosphors are 10 mol%. All the four charge compensators increase the luminescent intensity of $\text{SrB}_2\text{O}_4:\text{Tb}^{3+}$ phosphor. Especially, Na^+ ions exhibit the strongest charge compensation abilities. The order of charge compensation abilities is $\text{Na}^+ > \text{K}^+ > \text{Li}^+$. These phenomena may be attributed to the ionic radius size of Li^+ (59 pm), Na^+ (102 pm), K^+ (133 pm) and Sr^{2+} (113 pm). Compared with the radius of Li^+ and K^+ ion, Na^+ ionic radius is more similar to that of Sr^{2+} . Na^+ as charge compensator together with Tb^{3+} substituted two Sr^{2+} sites in SrB_2O_4 crystal lattice which would lead to a smaller lattice deformation than Li^+ and K^+ , so the $\text{Sr}_{0.80}\text{B}_2\text{O}_4:\text{Tb}^{3+}_{0.10},\text{Na}^+_{0.10}$ phosphor shows the strongest luminescent intensity. Similarly, the radius of K^+ ion is more closer to that of Sr^{2+} ion than Li^+ ion. So the $\text{Sr}_{0.80}\text{B}_2\text{O}_4:\text{Tb}^{3+}_{0.10},\text{K}^+_{0.10}$ shows a stronger luminescent intensity than $\text{Sr}_{0.80}\text{B}_2\text{O}_4:\text{Tb}^{3+}_{0.10},\text{Li}^+_{0.10}$.

The photograph of $\text{Sr}_{0.90}\text{B}_2\text{O}_4:\text{Tb}^{3+}_{0.10}$ (a), $\text{Sr}_{0.80}\text{B}_2\text{O}_4:\text{Tb}^{3+}_{0.10},\text{Li}^+_{0.10}$ (b), $\text{Sr}_{0.80}\text{B}_2\text{O}_4:\text{Tb}^{3+}_{0.10},\text{Na}^+_{0.10}$ (c) and $\text{Sr}_{0.80}\text{B}_2\text{O}_4:\text{Tb}^{3+}_{0.10},\text{K}^+_{0.10}$ (d) under ultraviolet light irradiation is also shown in inset of Fig. 6. It can be seen that all of the samples show bright green emission.

Table 1
CIE chromaticity coordinates and $^5\text{D}_4 \rightarrow ^7\text{F}_5$ relative emission intensity of phosphors.

| Phosphors | Emission wavelength (nm) | CIE chromaticity coordinates | | $^5\text{D}_4 \rightarrow ^7\text{F}_5$ relative intensity |
|---|--------------------------|------------------------------|------|--|
| | | x | y | |
| $\text{Sr}_{0.90}\text{B}_2\text{O}_4:\text{Tb}^{3+}_{0.10}$ | 544 | 0.27 | 0.53 | 1.00 |
| $\text{Sr}_{0.80}\text{B}_2\text{O}_4:\text{Tb}^{3+}_{0.10},\text{Li}^+_{0.10}$ | 544 | 0.27 | 0.57 | 2.80 |
| $\text{Sr}_{0.80}\text{B}_2\text{O}_4:\text{Tb}^{3+}_{0.10},\text{Na}^+_{0.10}$ | 544 | 0.27 | 0.59 | 4.36 |
| $\text{Sr}_{0.80}\text{B}_2\text{O}_4:\text{Tb}^{3+}_{0.10},\text{K}^+_{0.10}$ | 544 | 0.26 | 0.58 | 3.27 |

The PAL standard values $x = 0.29$, $y = 0.60$.

The order of luminescent intensity for the four phosphors is $c > d > b > a$ observed by naked eyes. The sequence is in accordance with the results measured by Fluorescence Spectrometer.

4. Conclusion

A new green-emitting phosphor of $\text{SrB}_2\text{O}_4:\text{Tb}^{3+}$ was prepared by conventional solid-state reaction at 800 °C and its photo-luminescence properties were studied. The phosphor $\text{SrB}_2\text{O}_4:\text{Tb}^{3+}$ exhibits bright green emission at 378 nm NUV light excitation. The critical quenching concentration of Tb^{3+} in $\text{SrB}_2\text{O}_4:\text{Tb}^{3+}$ phosphor is about 10 mol%. All the three charge compensations increased the luminescent intensity of $\text{SrB}_2\text{O}_4:\text{Tb}^{3+}$. Especially, Na^+ is the optimal charge compensator and the emitting intensity of the phosphor with Na^+ as charge compensator is 4.36 times as strong as the one without charge compensator. The reasons may be related to the relative size of Li^+ , Na^+ , and K^+ radius compared with Sr^{2+} . All the phosphors show excellent CIE chromaticity coordinates, especially that of $\text{Sr}_{0.80}\text{B}_2\text{O}_4:\text{Tb}^{3+}_{0.10}, \text{Na}^+_{0.10}$ which is more close to the phase alternation line (PAL) standard values ($x = 0.29$, $y = 0.60$). All the results indicate that the phosphor is a promising green phosphor pumped by NUV InGaN chip for fabricating WLED.

Acknowledgements

This work was financially supported by the National Natural Science Foundation of the People's Republic of China

(Nos. 20977055 and 21007029), the Natural Science Foundation of Shandong Province (ZR2012BQ017), Qingdao Project of Science and Technology (11-2-4-3-(16)-jch) and the Opening Foundations of State Key Laboratory of Geological Processes and Mineral Resources (Nos. GPMR201010 and GPMR201102).

References

- [1] P.L. Li, Z. Xu, S.L. Zhao, F.J. Zhang, Y.S. Wang, Mater. Res. Bull. (2012), <http://dx.doi.org/10.1016/j.materresbull.2012.03.060>.
- [2] X.S. Yan, W.W. Li, K. Sun, Mater. Res. Bull. 46 (2011) 87–91.
- [3] J. Liu, X.D. Wang, Z.C. Wu, S.P. Kuang, Spectrochim. Acta Part A 79 (2011) 1520–1523.
- [4] L.S. Zhao, J. Liu, Z.C. Wu, S.P. Kuang, Spectrochim. Acta Part A 87 (2012) 228–231.
- [5] C.F. Guo, X. Ding, H.J. Seo, Z.Y. Ren, J.T. Bai, Opt. Laser Technol. 43 (2011) 1351–1354.
- [6] Z.L. Wang, H.B. Liang, M.L. Gong, Q. Su, Electrochem. Solid State Lett. 8 (2005) H33–H35.
- [7] R. Wang, J. Xu, C. Chen, Mater. Lett. 68 (2012) 307–309.
- [8] J.L. Zhang, X.G. Zhang, M.L. Gong, J.X. Shi, L.P. Yu, C.Y. Rong, S.X. Lian, Mater. Lett. 79 (2012) 100–102.
- [9] P.A. Nagpure, S.K. Omanwar, J. Lumin. 132 (2012) 2088–2091.
- [10] A. Lakshmanan, R.S. Bhaskar, P.C. Thomas, R.S. Kumar, V.S. Kumar, M.T. Jose, Mater. Lett. 64 (2010) 1809–1812.
- [11] N. Xie, Y.L. Huang, X.B. Qiao, L. Shi, H.J. Seo, Mater. Lett. 64 (2010) 1000–1002.
- [12] P.L. Li, Z.J. Wang, Z.P. Yang, Q.L. Guo, X. Li, Mater. Lett. 63 (2009) 751–753.
- [13] P.L. Li, L.B. Pang, Z.J. Wang, Z.P. Yang, Q.L. Guo, X. Li, J. Alloys Compd. 478 (2009) 813–815.
- [14] P.L. Li, Z.J. Wang, Z.P. Yang, Q.L. Guo, G.S. Fu, Mater. Res. Bull. 44 (2009) 2071–2608.
- [15] G. Blasse, B.C. Grabmaier, Luminescent Materials, Springer, Berlin, 1994.
- [16] S. Shionoya, W.M. Yen, Phosphor Handbook, CRC Press, New York, 1999.